Defect states assisted charge conduction in Au/MoO_{3-x}/*n*-Si Schottky barrier diode

Somnath Mahato[¥§*], Cristobal Voz[§], Debaleen Biswas[¥] and Satyaban Bhunia[¥] Joaquim Puigdollers[§],

[¥]*Saha Institute of Nuclear Physics, Surface Physics and Material Science division, 1/AF Bidhannagar, Kolkata 700064, India*
[§]*Electronic Engineering Department, Polytechnic University of Catalonia, Barcelona 08034, Spain*

**Corresponding author's email: som.phy.ism@gmail.com*

Abstract: Role of defect states of thermally grown molybdenum trioxide (MoO_{3-x}) on electrical conductivity was investigated via low temperature current–voltage and capacitance–voltage measurements. To clarify the charge transport phenomena through MoO_{3-x}, a 15 nm thin layer of MoO_{3-x} film was used as an interface layer between gold and *n*-type Silicon (*n*-Si). The formations of interfacial dipole between *n*-Si and MoO_{3-x} interface exhibit a rectifying behaviour of Au/MoO_{3-x}/*n*-Si Schottky barrier diode (SBDs). The rectifying nature of the SBDs shown up to 175 K due to proper electron extraction from valence band to conduction band via the defect states; however at ≤165 K the rectifying nature was not observed due to insulating behaviour of MoO_{3-x} layer. Oxygen deficiency as a formation of defects was determined by X-ray photoelectron spectroscopy (XPS). Consequences of these defects as a function of current conduction across the MoO_{3-x} was also confirmed by low temperature photoluminescence (PL) measurement.

Metal–Oxide–Semiconductor (MOS) is the most useful device in the study of electrical properties of thin film semiconductors. Investigations of current conduction mechanism in Schottky barrier diode (SBDs) with a thin layer of oxide material incorporated between a metal and a semiconductor have a long history. In order to obtain a Schottky barrier height (SBH) with good rectifying behaviour, a thin interfacial layer is commonly placed between the metal and semiconductor. Attempts so far have been made to use of different transition metal oxide as an interface layer in many electronic devices and shown their effectively improvement of overall device performance.[1] Chen *et.al.* [2] reported the presence of a thin interface layer of molybdenum trioxide between the metal and semiconductor referred to as metal/oxide/semiconductors (MOS) like SBDs. This MOS device has become more popular compared with the other types of SBDs because of their many applications. [3,4]

Nowadays, the application of transitional metal oxides (TMOs) such as MoO_3, V_2O_5 and WO_3 are not only limited in organic electronics but also extended to the organic/inorganic optoelectronic devices. All these TMOs are being used as an ultra thin layer of alternative hole transport layer on crystalline silicon (c-Si) to achieved record efficiencies on heterojunction silicon solar cell. [5,6] In particular, Molybdenum trioxide (MoO_3) is a wide-band-gap (3.0 eV – 3.1 eV) semiconductor, with a large electron affinity (9.7 eV) [7] and high work function (5.5 eV) [8] material. James *et. al.* [9] reported that MoO_3 is a semiconductor with a very low conductivity (10^{-7} S/cm) whereas MoO_2 has high conductivity compare as a metal (10^4 S/cm).

Therefore, decrease of oxidation state of molybdenum cations ($MoO_3 \rightarrow MoO_2$) could cause a better electrical conductivity. Therefore, non-stoichiometric MoO_{3-x} thin film has good electrical conductivity and suitable for many optoelectronic device applications.[10] Recently, R. G. Hernansanz *et.al.* [11] explained the charge transport mechanisms through molybdenum oxide in silicon heterojunction solar cells.

In this letter, we have demonstrated the defects presence in thermally grown MoO_{3-x} thin film is the main contribution of charge transportations into MoO_{3-x} layer. First time we have reported, below a certain temperature (≤165 K), the MoO_{3-x} layer behaved as an insulator due to insufficient thermal energy to reach electrons from defect state to conduction band. In order to explain our observation, we fabricated Au/MoO_{3-x}/*n*-Si MOS SBDs and characterized by low temperature Current–Voltage (I–V) and Capacitance–Voltage (C–V) measurements. Calculated all Schottky parameters are successfully explained by thermionic emission (TE) theory.

N-type float zone with (100) oriented c-Si wafers were used as a substrate. Resistivity and thickness of the wafer was 2.4 Ω-cm and 280 μm respectively. The wafer was cleaning by RCA and dip into 1% HF for one minute. The back side was passivated with an hydrogenated amorphous silicon (a-Si:H) stack (5 nm intrinsic/15 nm *n*-doped) followed by a hydrogenated amorphous silicon carbide (a-SiC:H) back-reflection layer (80 nm), deposited by plasma-enhanced chemical vapor deposition (PECVD) (13.56 MHz, 300 °C). A nanosecond infrared laser was used to locally diffuse the *n*-dopant ensuring a very good ohmic contact with the e-beam evaporated Ti/Al electrode. [12] Then pure molybdenum trioxide powder (Sigma Aldrich, 99.99%) was thermally evaporated on the silicon substrate at pressure 10^{-6} mbar with the deposition rate 0.2Å/s. The thickness of MoO_3 thin film was 15 nm. Finally, high purity gold (50 nm) was deposited through a shadow mask. Figure 1 shows the energy band structure and schematic diagram and cross section FESEM image of Au/MoO_{3-x}/*n*-Si MOS SBDs.

The I–V and C–V measurements were performed by a Keithley 4200SCS semiconductor parameter analyzer and an Agilent E4980A LCR meter. A cryostat with a Lakeshore temperature controller was employed to perform the electrical characterization at different temperatures ranging from 300 K to 80 K. The photoluminescence spectra were taken in the temperature range of 25 K to 250 K using He–Cd laser as a light source with an excitation wavelength of 325 nm. The luminescence signal was analyzed and recorded through a monochromator equipped with a photomultiplier detector. Chemical composition of deposited MoO_{3-x} thin films were characterized by X-ray photoelectron spectroscopy (XPS) scans (SPECS system, Phoibos 150 detector, Germany at 3 $\times 10^{-9}$ mbar) from a MoO_{3-x}/*n*-Si (polished silicon) substrate using a non-monochromatic Al-Kα source. All binding energies were referred to the C1s energy level for internal reference. The reported binding energies were adjusted to correspond to the reference energies.

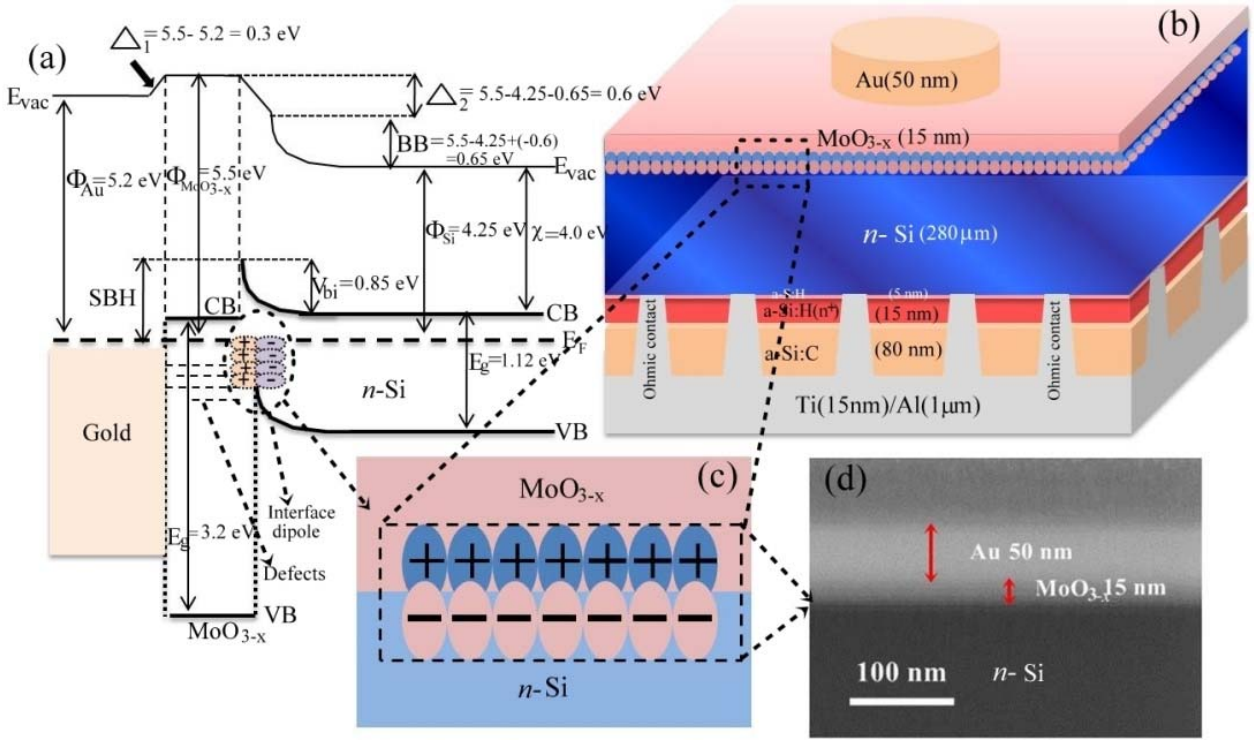

Figure 1: [(a) & (b)] Energy-band diagram and schematic sketched of the Au/MoO_{3-x}/*n*-Si MOS SBDs, whereas SBH is Schottky barrier height, BB is band banding, , ϕ_{Au} , ϕ_{MoO3-x} & ϕ_{Si} are the work function of gold, molybdenum trioxide & *n*-type Si and χ is the electron affinity. (c) Formation of interface dipole between MoO_{3-x} and *n*-Si. (d) Cross–section FESEM image of Au/MoO_{3-x}/*n*-Si SBDs.

Using Schottky–Mott relation at Au/MoO_{3-x} junction, $\phi_{bn} = \phi_{Au} - \chi_{MoO3-x}$ = (5.2 – 5.4) eV = – 0.2 eV, which is quite low, sufficing the practical purpose of ohmic contact. Whereas in MoO_{3-x}/*n*-Si contact using same Schottky-Mott relation, $\phi_{bn} = \phi_{MoO3-x} - \chi_{Si}$ = (5.5 – 4.0) eV = 1.5 eV is very high and which justifying the Schottky contact. Alternatively, if the work function of metal is greater than semiconductor ($\phi_m > \phi_S$), the junction behaves as a Schottky junction if not then it is ohmic. As, $\phi_{MoO3-x} > \phi_{Si}$ so the MoO_{3-x}/Si interface is mostly responsible for the rectifying nature whereas $\phi_{Au} < \phi_{MoO3-x}$ behaves as an ohmic contact. According to Kleider *et.al* [13], a strong charge inversion layer formed inside silicon surface due to high band offset between MoO_{3-x} and *n*-Si during thermal evaporation. The inversion layer acts as an interfacial dipole shown in figure 1(c), which could help to improve the rectifying nature of the SBDs. The dipoles are created due to internal layer structure of MoO_3 on *n*-Si substrate during deposition. [14,15] To clarify the interface layer, we deposited MoO_3 thin film by same evaporation on glass and silicon and calculated sheet resistance by transfer-length-method (TLM) shown in figure 2. The obtained sheet resistance of MoO_{3-x} film on glass is 5.04×10^{12} Ω/sq and on *n*-Si is 1.00×10^{4} Ω/sq. As it is seen, the sheet resistance on glass is several orders of magnitude higher than that of silicon substrate. That means the current do not flow only the MoO_{3-x} layer in case of silicon. Current can flow through three paths proposed in figure 2(b): (i) bulk silicon (ii) through

MoO_{3-x} layer or (iii) through a hypothetic inversion layer. For the silicon bulk path, the electron must cross an important barrier due to the silicon conduction band bending which makes the current flow though this path very unlikely. In MoO_{3-x} path, the calculated sheet resistance is very high (10^{12} Ω/sq) so the conductivity is very low. That means electron flow through MoO_{3-x} layer is quite less. Therefore, most of electrons are flow through the alternative path constitute by the inversion layer.

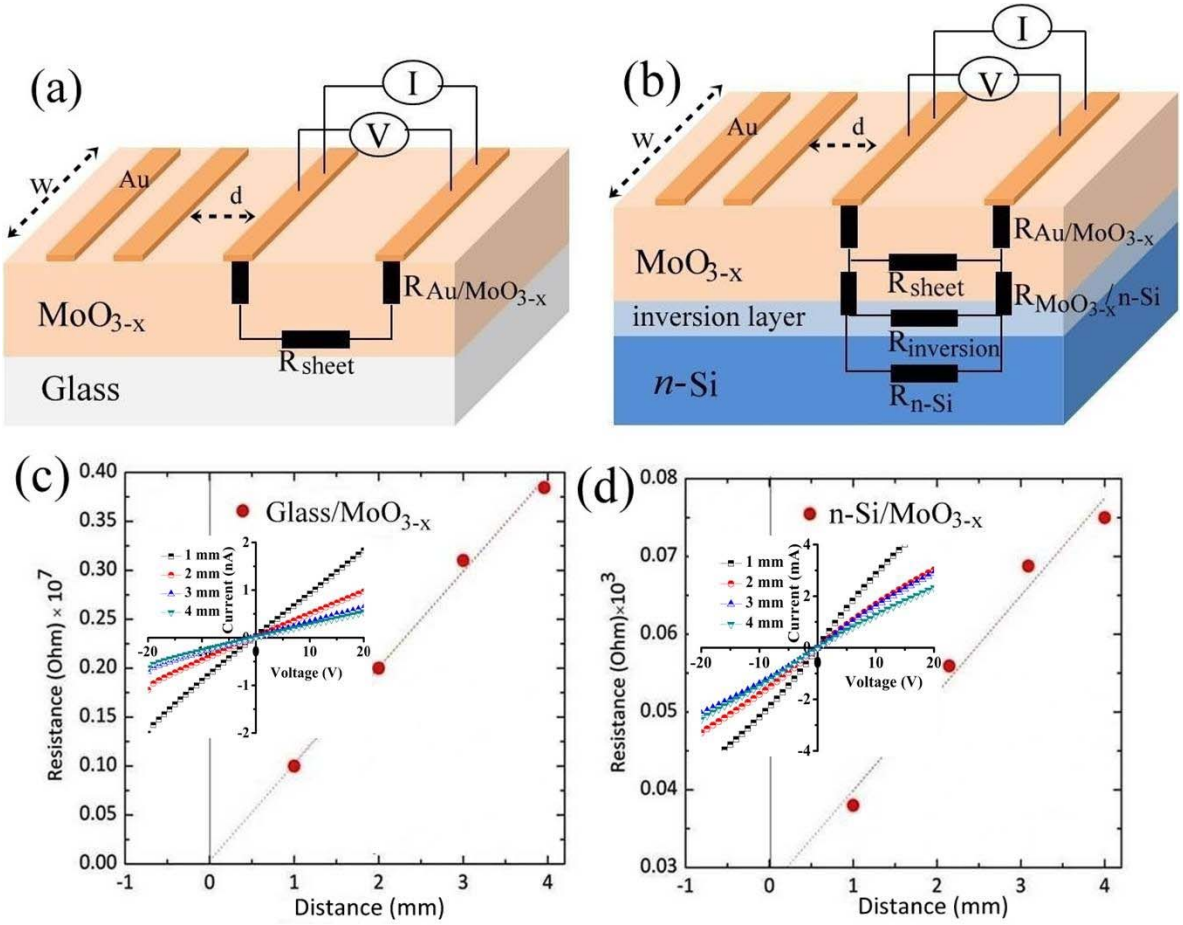

Figure 2: Schematic diagram of different current configurations on (a) glass and (b) *n*-Si. [(c) and (d)] TLMs of MoO_{3-x} films over a glass and *n*-Si substrate. (Insets) I–V measurements at different distance and the sample geometry.

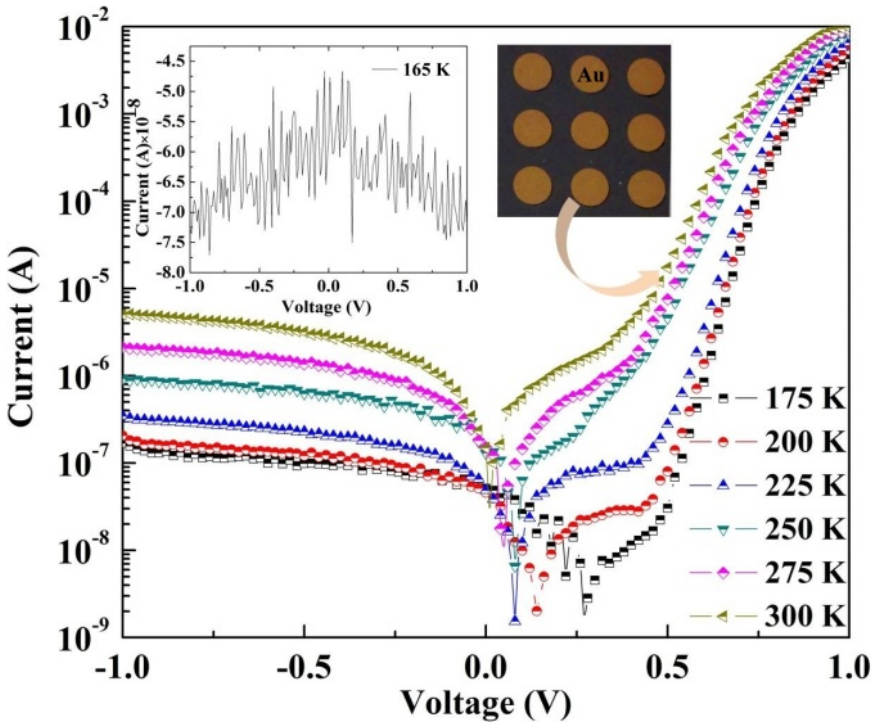

Figure 3: Temperature dependent Current–Voltage (I–V) characteristics and (inset) I–V at 165 K and top view photography of Au/MoO_{3-x}/*n*-Si MOS SBDs.

Figure 3 shows the temperature dependent I–V characteristics of Au/MoO_{3-x}/*n*-Si MOS SBDs. The rectifying nature of the SBDs is observed upto 175 K. According to TE theory *I–V* characteristics of a SBDs is given by [16]

$$I = AA^{*}T^{2}\, exp\left(-\frac{q\varphi_{bo}}{KT}\right)\left[\exp\left(\frac{qV}{nkT}\right)-1\right] \qquad (1)$$

where *A*, ϕ_{b0}, *q*, *V*, *n*, *k* and *T* is the diode area, barrier height (BH), electron charge, forward–bias voltage, ideality factor, Boltzmann constant and temperature in Kelvin respectively. A^{*} is the Richardson constant which is expressed as $A^{*} = \frac{4\pi q m^{*} K^{2}}{h^{3}}$ and its estimated value is 120 A–cm^{-2}–K^{-2} for *n*-type Silicon. [17] From the intercept and slope of *lnI* vs. *V* plot, the value of ϕ_{b0} and *n* at each temperature were extracted. The obtained ϕ_{b0} increased and *n* decreased with the increase of temperature, as shown in figure 4(a). Simultaneously, the ϕ_{b0} values are estimated from temperature dependent C–V measurements. More details calculation about barrier height from C–V measurements can be found in our previous works. [18] Calculated barrier height from *C–V* measurements is higher than the value of barrier height estimated from the *I–V* measurements as excepted. [19] Therefore the obtained barrier height from the C–V doesn't correspond to the I–V measurements and the ideality factor (*n*) is always >1. This discrepancy indicates the existence of inhomogeneity [20,21] or excess capacitance [22] at the interface due to an ultra thin (~2 nm) silicon suboxide (SiO_x) layer [6] is automatically grown on the silicon substrate due to the interaction between MoO3-x layer and the crystalline silicon or current tunneling through the

interface as used highly doped *n*-type Si substrate or generation recombination of electrons within the space charge limited region.

The second way to evaluate the barrier height in forward bias region is using the conventional Richardson plot, which can be written as: [23]

$$ln\left(\frac{I_0}{T^2}\right) = ln(AA^*) - \frac{q\phi_{b0}}{kT} \qquad (2)$$

where the variation of $ln(I_0/T^2)$ vs. $1000/T$ is found to be linear in the temperature range from 300 K to 175 K. From the best linear fit of Richardson plot (figure 4(c)), activation energy (E_a) and Richardson constant (A^*) are evaluated. The calculated E_a is 1.85 eV, which is large compared to the bandgap of *n*-Si. In addition, the Richardson constant is 112.43×10^{-4} A–cm^{-2}–K^{-2}, which is very low compared to the known theoretical value of *n*-Si. This above abnormal behavior may be affected by the inhomogeneity. To explain such kind of abnormal nature we have assumed the double Gaussian distribution of apparent BH using potential fluctuation model. [24, 25] This model is based on inhomogeneous BH at the interface where n_{ap} and ϕ_{ap} are the apparent ideality factor and barrier height at zero bias voltage. By linear fitting of the experimental data of ϕ_{ap} vs. 1000/T (figure 4(d)) should be a straight line with the intercept gives the zero-bias mean barrier height ($\overline{\phi_{b0}}$) = 1.33 eV and the slope giving the zero-bias standard deviation (σ_0) = 0.136 V. This value of σ_0 is not a small value compared to $\overline{\phi_{b0}}$ which indicates the existence of inhomogeneities at the interface. Plot of $1/n_{ap}$ vs. 1000/T should also a straight line and intercept and slope gives the voltage coefficient ρ_2 = 0.046 V and ρ_3= – 0.205 V. Hence, we may conclude that the linear behaviour indicates a double Gaussian distribution in Schottky barrier diodes. Using the standard deviation, modified Richardson equation can be expressed as: [17]

$$ln\left(\frac{I_0}{T^2}\right) - \frac{q^2\sigma_0^2}{2k^2T^2} = ln(AA^*) - \frac{q\overline{\phi_{b0}}}{kT} \qquad (3)$$

According to the modified Richardson plot $ln(I_0/T^2) - (q\sigma)^2/2(kT)^2$ vs. $1000/T$ should give straight line (figure 4(e)) whose slope directly yields the mean barrier height ($\overline{\phi_{b0}}$) and intercept ($=lnAA^*$) determined A^* value for a given diode area A. The calculated ($\overline{\phi_{b0}}$) = 1.33 eV from modified Richardson plot is exactly same as the value evaluated from ϕ_{ap} vs. $1000/T$ plot. However, the evaluated zero bias barrier height and mean barrier height is higher than that of actual silicon bandgap. This deviation may be the effect of inhomogeneity or the interfacial layer or interface states such as semiconductor surface states, formation of interface dipole, defects or dislocations. Subsequently, A^* = 155.18 A–cm^{-2}K^{-2} is very close to the known theoretical value of *n*-Si. Thus, the inhomogeneity not only affects the I–V but also the C–V characteristics. It has been demonstrated that the capacitance depends on the standard deviation of the barrier distribution. Thus, the difference between ϕ_{C-V} and ϕ_{I-V} can be assumed as a Gaussian distribution of BH, which may be represented as: [26]

$$\phi_{C-V} - \phi_{I-V} = \frac{q\sigma_0^2}{2kT} + \frac{q\sigma_0\alpha_\sigma}{2k} \qquad (4)$$

where α_σ is the temperature dependent coefficient of σ_0. Experimental plot of $\phi_{C-V} - \phi_{I-V}$ vs. 1000/T (figure 4(f)) should give a straight line whose slope and intercept are $\frac{q\sigma_0^2}{2k}$ and $\frac{q\sigma_0\alpha_\sigma}{2k}$ respectively. The calculated σ_0 is 0.137 V which corroborates our above calculation. Therefore, the presence of inhomogeneity plays an important role in MOS SBDs device performance and in the analysis of the electrical parameters. To understand the proper charge transport phenomena of Au/MoO_{3-x}/*n*-Si SBDs device can be obtained from Log(I)–Log(V) plot of temperature dependent I–V curve shown in figure 5(a). At low voltage, the slope of the curves are < 2 which represents the ohmic nature of the device for all temperatures. But, at high voltage region the slopes are >> 2. In this case, injection of charge carriers through the traps or defects occurred and increased considerably. Thus the charge transportations through MoO_{3-x} layer is controlled by traps charge or defects which is known as trapped charge limited current (TCLC).

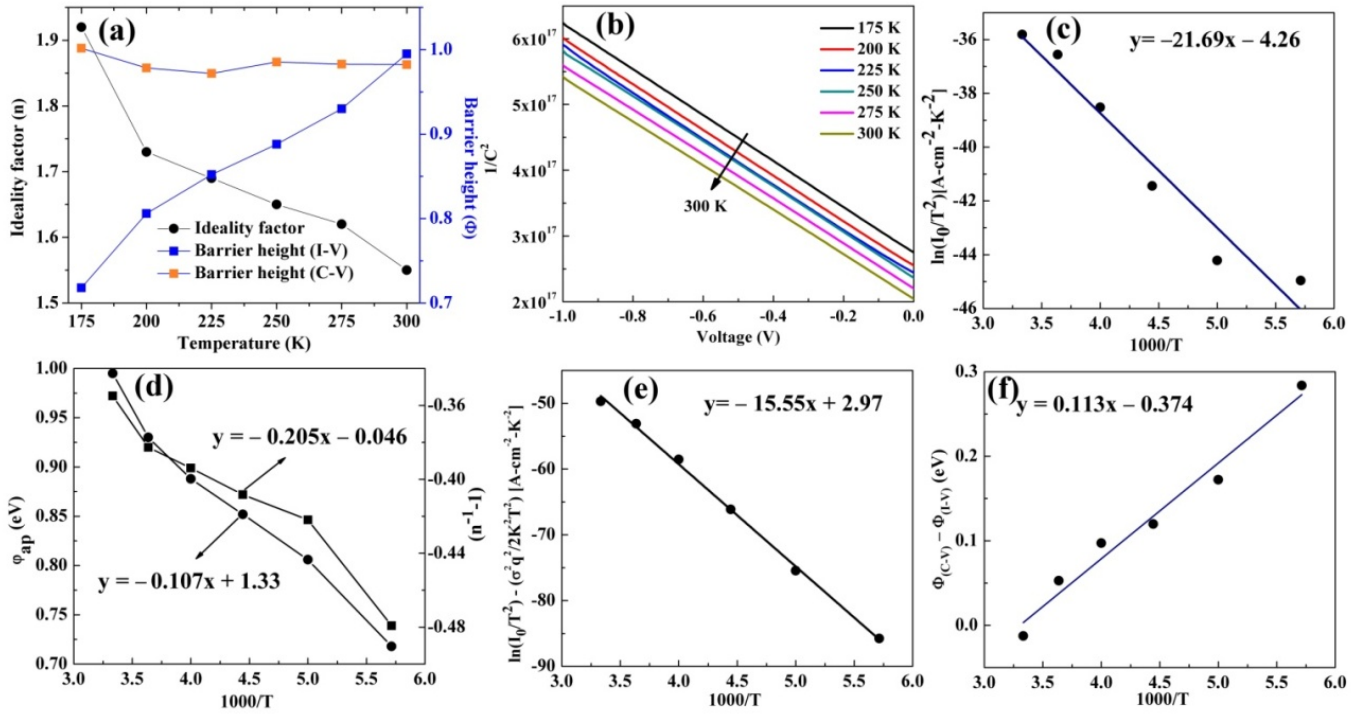

Figure 4: (a) Ideality factor (*n*) and barrier height (ϕ) plot calculated from I–V and C–V measurements, (b) Temperature dependent $1/C^2$ vs. V plot of the Au/MoO_{3-x}/*n*-Si MOS SBDs (c) Richardson plots of the $ln(I_0/T^2)$ vs. *1000/T* (d) ϕ_{ap} vs. *1000/T* and $((1/n_{ap}) - 1)$ vs. *1000/T* curves for the SBDs at the temperature range from 300 K to 175 K (e) Modified Richardson $ln(I_0/T^2) - (q\sigma)^2/2(kT)^2$ vs. *1000/T* plot and (f) $\phi_{C-V} - \phi_{I-V}$ vs. 1000/T curve according to the double Gaussian distribution barrier heights.

To confirm the defects in thermally grown MoO_3 thin film, we characterized a wide range of (0 - 1200 eV) XPS spectrum of MoO3 film deposited on *n*-Si (100) surface shown in figure 5(b). The spectrum shows that the main constituent

elements of the film are molybdenum (Mo) and oxygen (O) atom. [27,28,29] The O 1s spectrum of MoO_{3-x} film consists of two components. The first component occurs on the low binding energy (531.3 eV) of the spectrum which can be assigned to the oxygen atom forming strong Mo=O bond in the oxide. The second O 1s peak, located at higher binding energy (532.5 eV), corresponds to oxide impurities accumulated in the film surface. Figure 5(c) shows the XPS 3d core level spectrum consists of two sublevels $3d_{3/2}$ and $3d_{5/2}$ due to spin–orbit splitting. Due to reactive interfaces, the Mo^{6+} cation of MoO_3 is reduced to Mo^{5+} and interfacial reduction of Mo^{6+} state to Mo^{5+} state is apparent from the XPS spectra. In MoO_3 oxide, oxidation state of Mo^{6+} for $3d_{5/2}$ and Mo $3d_{3/2}$ levels correspond to the binding energy of 233.4 eV and 236.5 eV and oxidation state of Mo^{5+} for $3d_{5/2}$ and $3d_{3/2}$ levels are in 231.7 eV and 234.9 eV, respectively. Now due to lack of oxygen, the molecular formula should be changed from MoO_3 to MoO_{3-x}. The value of 'x' is approximately 0.5. This oxygen deficiency acts as defect states in MoO_{3-x} thin film. As a result, electrons can easily jump from valence band to conduction band via the defect states. Hence, the defects are responsible for the current conduction in the MoO_{3-x} thin film.

The temperature dependence of Photoluminescence (PL) provides the confirmation about the defects in MoO_{3-x} thin film. [30,31] Figure 5(d) depicts the variation of PL intensity with wavelength at different temperatures. At very low temperatures (≥25K), excitonic lines are narrow and sharp. The peaks at 387nm (3.20 eV) 410 nm (3.02 eV) and 425 nm (2.91 eV) correspond to the band-to-band transitions and defects transition. But at higher temperature (≥175 K) defect-related bands are commonly broad because of the strong electron-phonon coupling due to thermal emission. Therefore, at very low temperature, electrons are quickly captured by positively charged shallow donors, while holes are mostly captured by negatively charged acceptors. For that at low temperatures, the probability of the donor acceptor recombination is much higher than the probability for electron to be captured directly by a neutral acceptor because the concentration of free electrons is much lower than the concentration of electrons bound to shallow donors and the current conduction is zero. When the temperature is increased the defect states at 425 nm (25 K) are shifted towards the higher wavelength at 438 nm (≥175 K) as well as several inactive defects are active with the increased of temperature due to broad PL spectrum (or continuous PL spectrum). The quenching of these PL bands is attributed to the thermal emission of electrons from the valence band to conduction band through the defect states. Which is signifying that above a certain temperature (≥175 K), the charge carriers can be achieved sufficient energy to rich valance band from defect states. This continuous defect is mainly responsible for the current conduction in MoO_{3-x} thin film, which is justified by our I-V measurement.

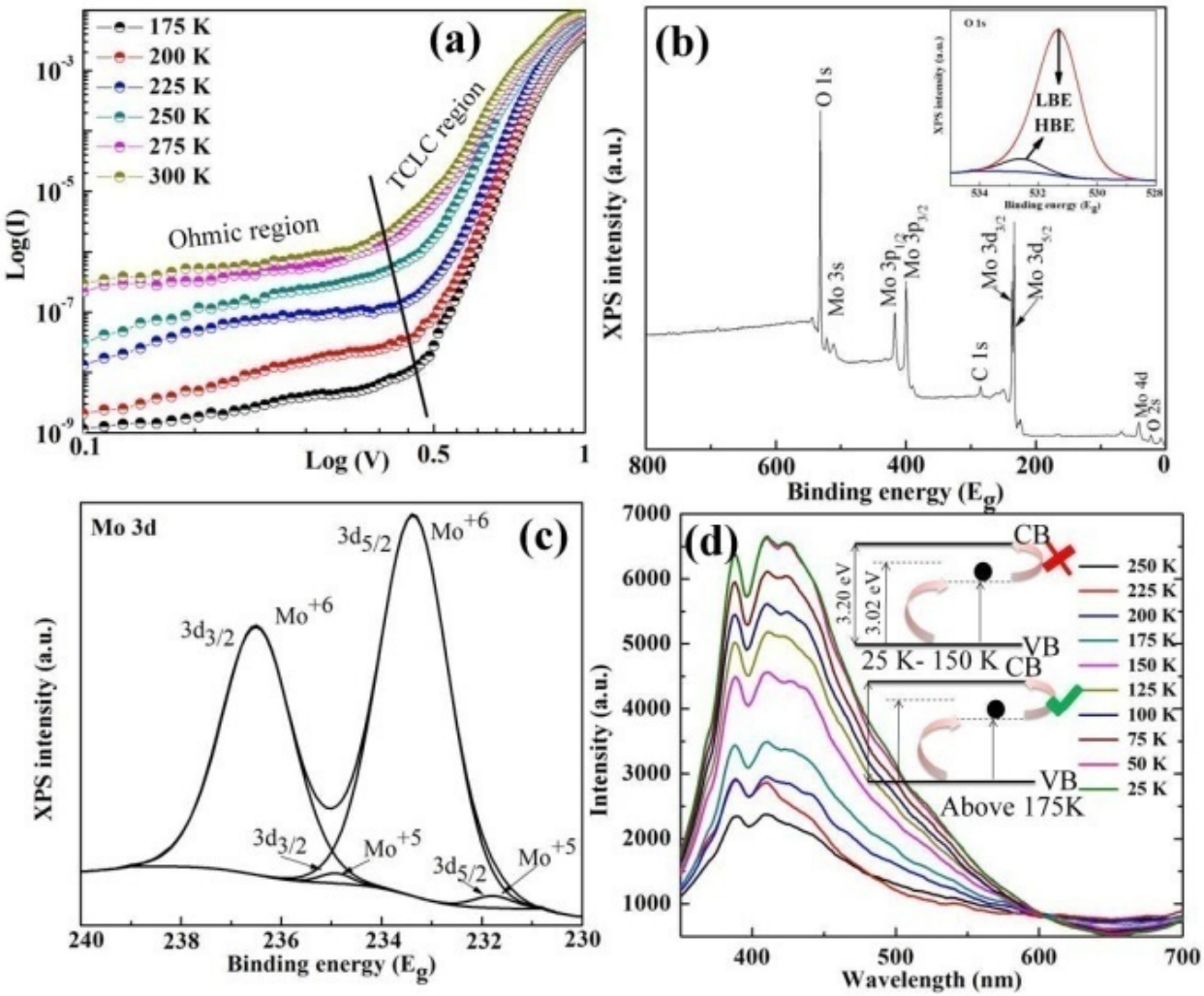

Figure 5: (a) Forward bias log(I)–log(V) graph from 175K to 300K and (b) General scan of high-resolution core level XPS spectra of MoO_{3-x} thin film (inset) deconvolution of O 1s core level of LBE and HBE components, (c) Mo $3d_{5/2}$ and Mo $3d_{3/2}$ peaks of a pristine MoO_{3-x} layer thermally deposited on *n*-Si. (d) Low temperature Photoluminescence measurements of MoO_{3-x} thin film excited at 325 nm.

In summary, molybdenum trioxide was reduced oxidation state of Mo from Mo^{+6} to Mo^{+5} convert to non-stoichiometric MoO_{3-x} thin film during the thermal evaporation process. The reduced oxidation generates the number of defects between valance and conduction band is responsible for the charge transportation. Low temperature PL measurement justified the defects present in MoO_{3-x} layer and shifted towards the higher wavelength with the increase of temperature. We first time investigated, at ≤165K $MoO3_{-x}$ layer behaves as an insulator due to insufficient thermal energy of electrons. The I–V–T results shown, the barrier height increased with increased of temperature but in C–V–T shown inverse characteristics. This discrepancy corresponds to the barrier inhomogeneity presence at the interface, which is liable for the deviation of device performance. The

modified Richardson plot considering by double Gaussian distribution of SBDs gives the Richardson constant of 155 A–cm^{-2} K^{-2} close to the known theoretical value for *n*-Si i.e. well justified by TE theory.

The work was financially supported by Erasmus Mundus Action 2 AREAS+ grant programs 2014-2015. Authors are thankful to Dr. Luis Guillermo Gerling and Mr. DUC Thomas of Department of Electronic Engineering, Universitat Politècnica de Catalunya Barcelona, Spain for their support. Authors are grateful to Dr. Supratic Chakraborty and Mr. Anway Pradhan of Saha Institute of Nuclear Physics, Kolkata, India for their assistance in electrical and photoluminescence measurements.

References

[1]R. Priya, M. S. Raman, N. S. Kumar, J. Chandrasekaran and R. Balan, *Optik* **127,** 7913 (2016)
[2]J. Chen, J. Lv, Q. Wang, *Thin Solid Films* **616,** 145 (2016)
[3]S. H. S. Chan, T. Y. Wu, J. C. Juan and C. Y. Teha, *Journal of Chemical Technology and Biotechnology* **86,** 1130 (2011)
[4]F. Yakuphanoglu, and B. F. Şenkal, *Journal of Physical Chemistry C* **111,** 1840 (2007)
[5]L.G. Gerling, S. Mahato, A. M. Vilches, G. Masmitja, P. Ortega, C. Voz, R. Alcubilla, J. Puigdollers, *Solar Energy Materials & Solar Cells* **145**, 109 (2016)
[6]G. Masmitjà, L. G. Gerling, P. Ortega, J. Puigdollers, I. Martín, C. Voz and R. Alcubilla, *Journal of Materials Chemistry A* **5,** 9182 (2017)
[7]J. Meyer, S. Hamwi, M. Kröger, W. Kowalsky, T. Riedl and A. Kahn, *Advanced Materials* **24**, 5408 (2012)
[8]P. Schulz, J. O. Tiepelt, J. A. Christians, I. Levine, E. Edri, E. M. Sanehira, G. Hodes, D Cahen and A Kahn, *ACS Applied Materials & Interfaces* **8**, 31491 (2016)
[9]J. Bullock, A. Cuevas, T. Allen and C. Battaglia, *Applied Physics Letters* **105,** 232109 (2014)
[10]Y. Guo, and J. Robertson, *Applied Physics Letter* **105,** 222110 (2014)
[11] R. García-Hernansanz, E. García-Hemme, D. Montero, J. Olea, A. del Prado, I. Mártil, C. Voz, L.G. Gerling, J. Puigdollers and R. Alcubilla, *Solar Energy Materia and Solar Cells* **185**, 61 (2018)
[12] P. Ortega, A. Orpella, I. Martín, M. Colina, G. López, C. Voz, M. I. Sánchez, C. Molpeceres and R. Alcubilla, *Progress in Photovoltaics: Research and Application* **20,** 173 (2012)
[13] J. P. Kleider, A. S. Gudovskikh, and P. Roca i Cabarrocas, *Applied Physics Letters* **92**, 162101 2008
[14]C. S. Lee, J. X. Tang, Y. C. Zhou and S. T. Lee, *Applied Physics Letters* **94,** 113304 (2009)
[15]X. Wang, K. Han, W. Wang, S. Chen, X. Ma, D. Chen, J. Zhang, J. Du, Y. Xiong and A. Huang, *Applied Physics Letters* **96.** 152907 (2010)
[16]J. J. Zeng and Y. J. Lin, *Applied Physics Letter* **104,** 133506 (2014).
[17]M. A. Yeganeh and S. H. Rahmatollahpur, *Journal of Semiconductors* **31,** 074001 (2010).
[18]S. Mahato, D. Biswas, L. G. Gerling, C. Voz and J. Puigdollers, *AIP Advances* **7,** 085313 (2017)
[19] Ö. Demircioglu, Ş. Karatas, N. Yıldırım, Ö. F. Bakkaloglu and A. Türüt, *Journal of Alloys and Compounds* **509** 6433 (2011)
[20]Z. Tekeli, Ş. Altındal, M. Çakmak, and S. Özçelik, *Journal of Applied Physics* **102,** 054510 (2007)
[21]Y. Li, W. Long and R. T. Tung, *Applied Physics Letters* **101,** 051604 (2012)
[22]M. Sharma and S. K. Tripathi, *Journal of Applied Physics* **112,** 024521 (2012)
[23]A. Elhaji, J. H. E. Freeman, M. M. El-Nahass, M. J. Kappers, C. J. Humphries, *Materials Science in Semiconductor Processing* **17,** 94 (2014)
[24]A. Gümüş, A. Türüt and N. Yalçin, *Journal of Applied Physics* **91,** 245 (2002)
[25]A. F. Özdemir, A. Turut and A. Kökçe, *Semiconductor Science and Technology* **21,** 298 (2006)
[26] H. Cetin and E. Ayyildiz, *Semiconductor Science and Technology* **20** 625 (2005)
[27]R. Ji, J. Cheng, X. Yang, J. Yu and L. Li, *RSC Advances* **7,** 3059 (2017)
[28]M. F. Al-Kuhaili, S. H. A. Ahmad, S. M. A. Durrani, M. M. Faiz, A. Ul-Hamid, *Materials and Design* **73,** 15 (2015)
[29]Y. Du, H. Y. Peng, H. Mao, K. X. Jin, H. Wang, F. Li, X. Y. Gao, W. Chen, and T. Wu, *ACS Applied Materials & Interfaces* **7**, 11309 (2015)
[30]M. A. Reshchikov, *Journal of Applied Physics* **115,** 012010 (2014)
[31]M. A. Reshchikov and H. Morkoç, *Journal of Applied Physics* **97,** 061301 (2005)